Wang et al., http://www.jcb.org/cgi/content/full/jcb.201507023/DC1

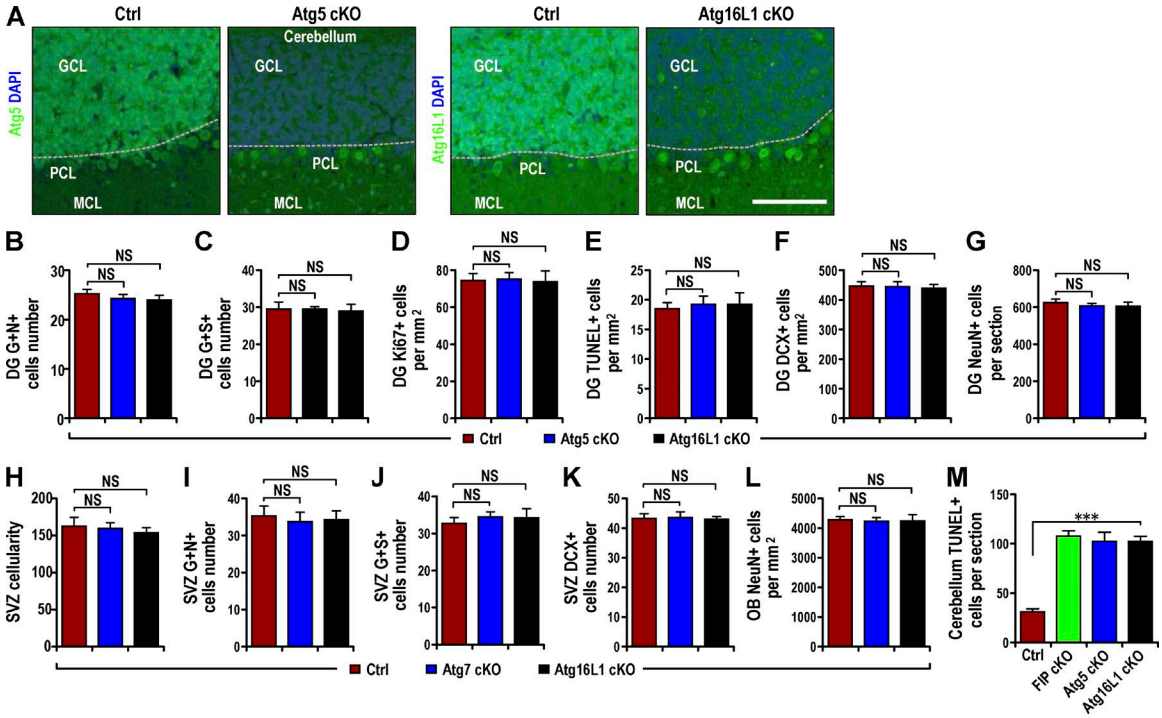

Figure S1. **Deletion of Atg5, Atg16L1, or Atg7 does not affect postnatal neural stem cells in the SGZ.** (A) Immunofluorescence of Atg5 (left), Atg16L1 (right), and DAPI in the cerebellum of Ctrl, *Atg5*^{GFAP} cKO, and *Atg16L1*^{GFAP} cKO mice at P28. Dotted lines indicate the boundary of granular cell layers. (B–G) Mean ± SEM of the number of positive cells per DG (B, C, and G) or per square millimeter of DG area (D–F) for GFAP and Nestin (B), GFAP and SOX2 (C), Ki67 (D), TUNEL (E), DCX (F), and NeuN (G) of Ctrl, *Atg5*^{GFAP} cKO, and *Atg16L1*^{GFAP} cKO mice at P28 (n = 4 mice for each). (H) H&E staining of the SVZ from Ctrl, *Atg16L1*^{GFAP} cKO, and *Atg7*^{UBC} cKO mice at P90. Mean ± SEM of SVZ cellularity per section is shown (n = 4 mice each). (I–L) Mean ± SEM of the number of positive cells for GFAP and Nestin (I), GFAP and SOX2 (J), and DCX (K) per SVZ section (I–K), and NeuN-positive cells per square millimeter of OB area (L) of Ctrl, *Atg16L1*^{GFAP} cKO, and *Atg7*^{UBC} cKO mice at P90 (n = 4 mice each). (M) Mean ± SEM of the TUNEL$^+$ cell number per section of Ctrl, *FIP200*^{GFAP} cKO, *Atg5*^{GFAP} cKO, and *Atg16L1*^{GFAP} cKO mice at P28 (n = 3 mice each). GCL, granular cell layer; MCL, molecular cell layer; PCL, Purkinje cell layer. Bars, 50 µm. ***, P < 0.001.

THE JOURNAL OF CELL BIOLOGY

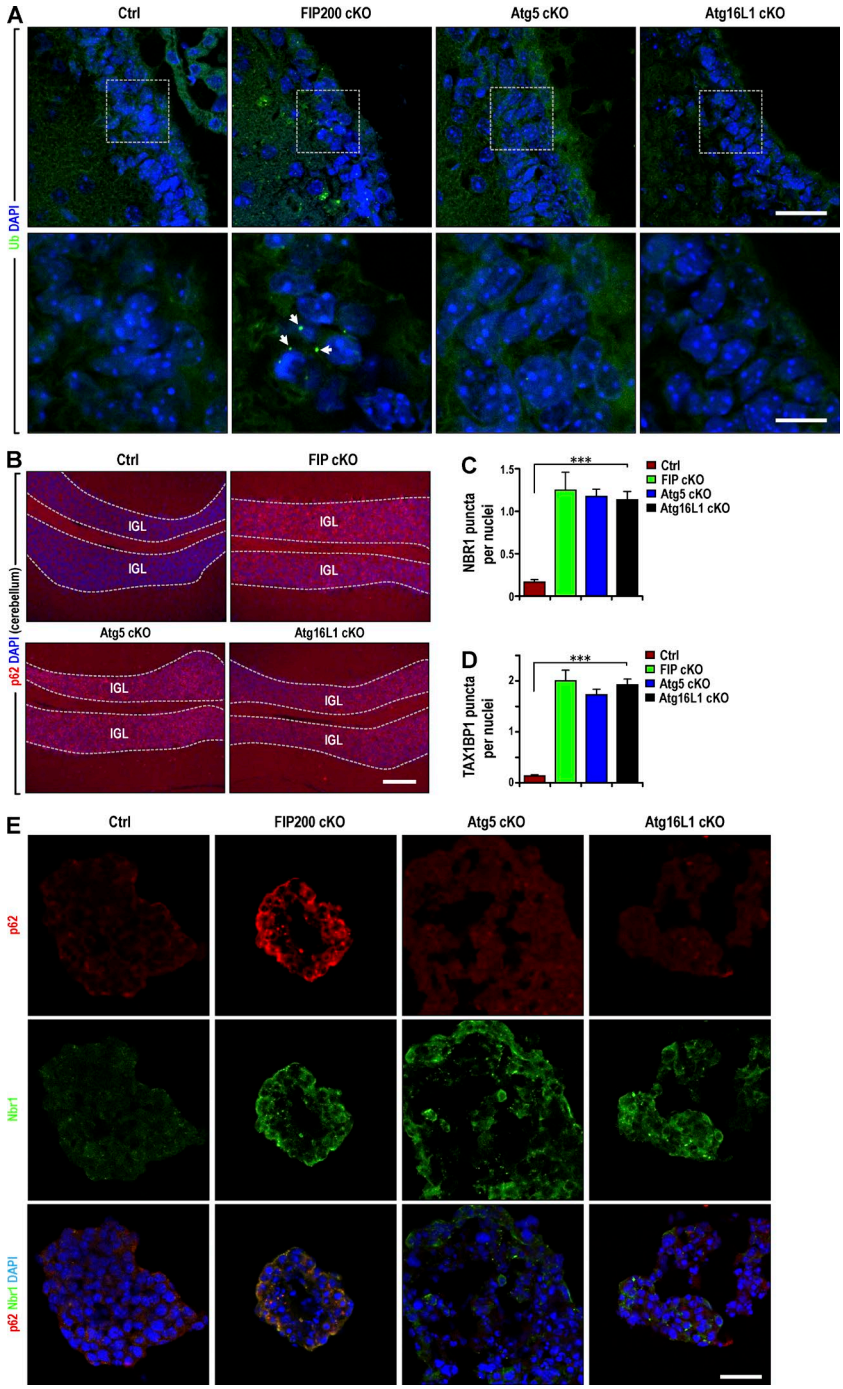

Figure S2. **Analyses of ubiquitin, p62, TAX1BP1, and NBR1 aggregates in *Fip200*^{GFAP} cKO, *Atg5*^{GFAP} cKO and *Atg16L1*^{GFAP} cKO mice.** (A) Immunofluorescence of ubiquitin and DAPI in the SVZ of Ctrl, *Fip200*^{GFAP} cKO, *Atg5*^{GFAP} cKO, and *Atg16L1*^{GFAP} cKO mice at P28. Boxed areas in upper panels are shown in more detail in lower panels. Arrows mark examples of ubiquitin-positive aggregates. (B) Immunofluorescence of p62 and DAPI in the cerebellum of Ctrl, *Fip200*^{GFAP} cKO, *Atg5*^{GFAP} cKO, and *Atg16L1*^{GFAP} cKO mice at P28. Dotted lines indicate the boundaries of IGL. (C and D) Mean ± SEM of the number of NBR1 (C) and TAX1BP1 aggregates (D) per neurosphere cell from Ctrl, *Fip200*^{GFAP} cKO, *Atg5*^{GFAP} cKO, and *Atg16L1*^{GFAP} cKO mice at P28 (n = 4 each). (E) Immunofluorescence of p62, NBR1 and DAPI in neurospheres from Ctrl, *Fip200*^{GFAP} cKO, *Atg5*^{GFAP} cKO, and *Atg16L1*^{GFAP} cKO mice at P28. IGL, internal granular layer. Bars: (A [top] and B) 50 µm; (A, bottom) 15 µm; (E) 20 µm. ***, P < 0.001.

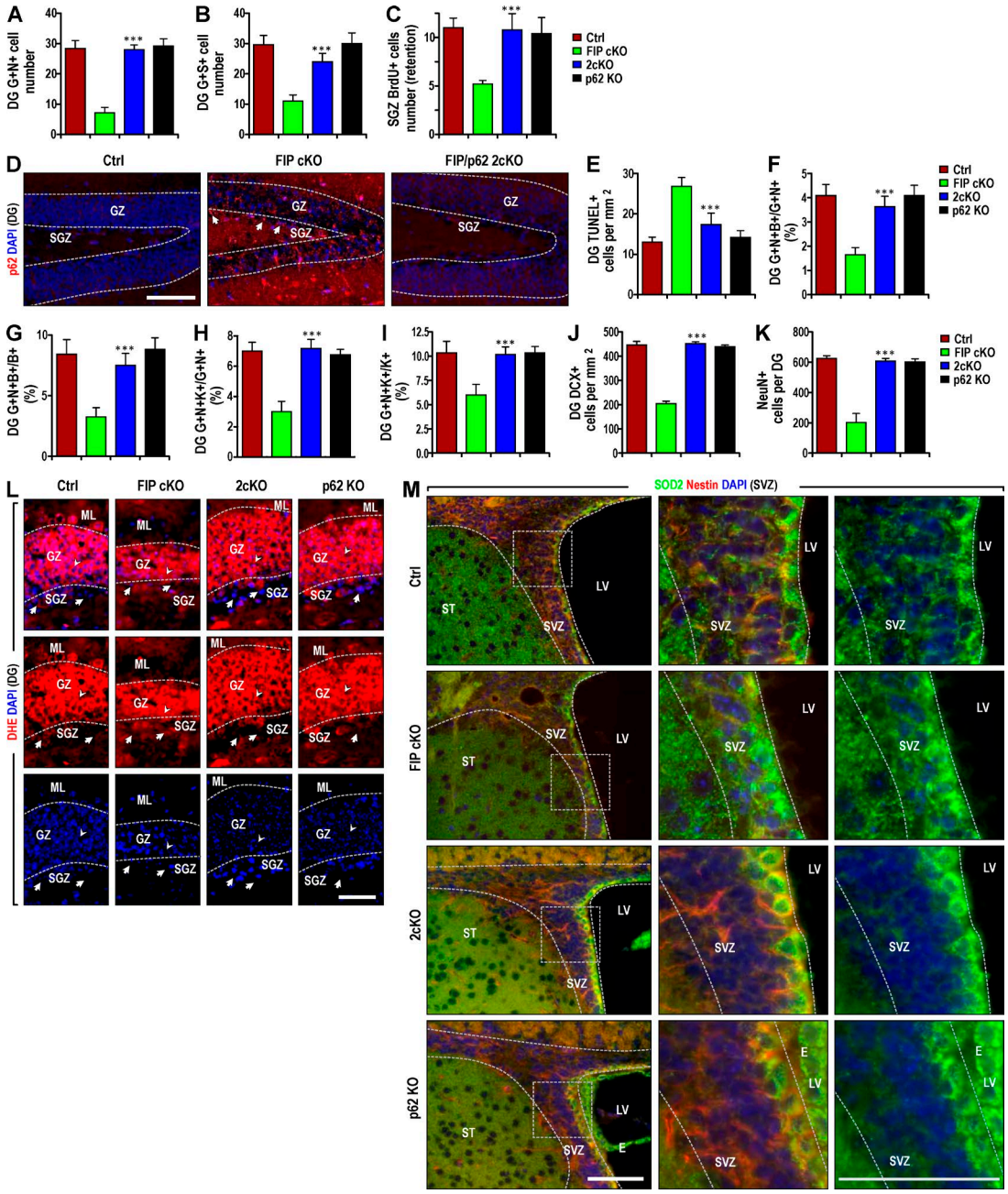

Figure S3. **p62 KO rescues degenerative neural stem cells in the SGZ of *Fip200*^{GFAP} cKO mice.** (A and B) Immunofluorescence of GFAP$^+$Nestin$^+$ (A) or GFAP$^+$Sox2$^+$ (B) cells in the DG of Ctrl, *Fip200*^{GFAP} cKO, 2 cKO, and p62 KO mice at P28. Mean ± SEM of the GFAP$^+$Nestin$^+$ cell number (A) and the GFAP$^+$Sox2$^+$ cell number (B) per SVZ section are shown (n = 4 for each). (C) Immunofluorescence of long-term retained BrdU and DAPI in the SGZ from Ctrl, *Fip200*^{GFAP} cKO, 2cKO, and p62 KO mice at P28. Mean ± SEM of the BrdU+ cell number per SGZ section is shown (n = 4 mice each). (D and E) Immunofluorescence for p62 and DAPI (D) and TUNEL and DAPI (E) in the SGZ of Ctrl, *Fip200*^{GFAP} cKO, 2cKO, and p62 KO mice at P28. Mean ± SEM of the fraction of TUNEL+ cells per square millimeter of DG area is shown in E (n = 3 mice for each). (F and G) Immunofluorescence for Nestin, GFAP, and short term labeled BrdU in the SGZ from Ctrl, *Fip200*^{GFAP} cKO, 2cKO, and p62 KO mice at P28. Mean ± SEM of the percentage of GFAP$^+$Nestin$^+$BrdU$^+$ of total GFAP$^+$Nestin$^+$ cells (F) or total BrdU$^+$ cells (G) per section are shown (n = 5 mice each). (H and I) Immunofluorescence for Nestin, GFAP, and Ki67 in the SGZ from Ctrl, *Fip200*^{GFAP} cKO, 2cKO, and p62 KO mice at P28. Mean ± SEM of the percentage of GFAP$^+$Nestin$^+$Ki67$^+$ of total GFAP$^+$Nestin$^+$ cells (H) or total Ki67$^+$ cells (I) per section are shown (n = 4 mice each). (J and K) Immunofluorescence for DCX (J) and NeuN (K) in the DG of Ctrl, *Fip200*^{GFAP} cKO, 2cKO, and p62 KO mice at P28. Mean ± SEM of DCX$^+$ (J) per square millimeter of DG area and NeuN$^+$ (K) cell number per DG are shown (n = 4 mice each). (L) Fluorescence of DHE and DAPI in the DG of Ctrl, *Fip200*^{GFAP} cKO, 2cKO, and p62 KO mice at P28. Arrows indicate SGZ cells, and arrowheads indicate granular neurons in the DG (n = 3 mice for each). (M) Immunofluorescence for Nestin, SOD2, and DAPI in the SVZ from Ctrl, *Fip200*^{GFAP} cKO, 2cKO, and p62 KO mice at P28. Boxed areas in the left column are shown in more detail in the middle and right columns. Dotted lines indicate the boundaries of the SVZ (M) and GZ (D and L). E, ependymal layer; LV, lateral ventricle; ML, molecular layer; ST, striatum. Bars, 50 µm. ***, P < 0.001.

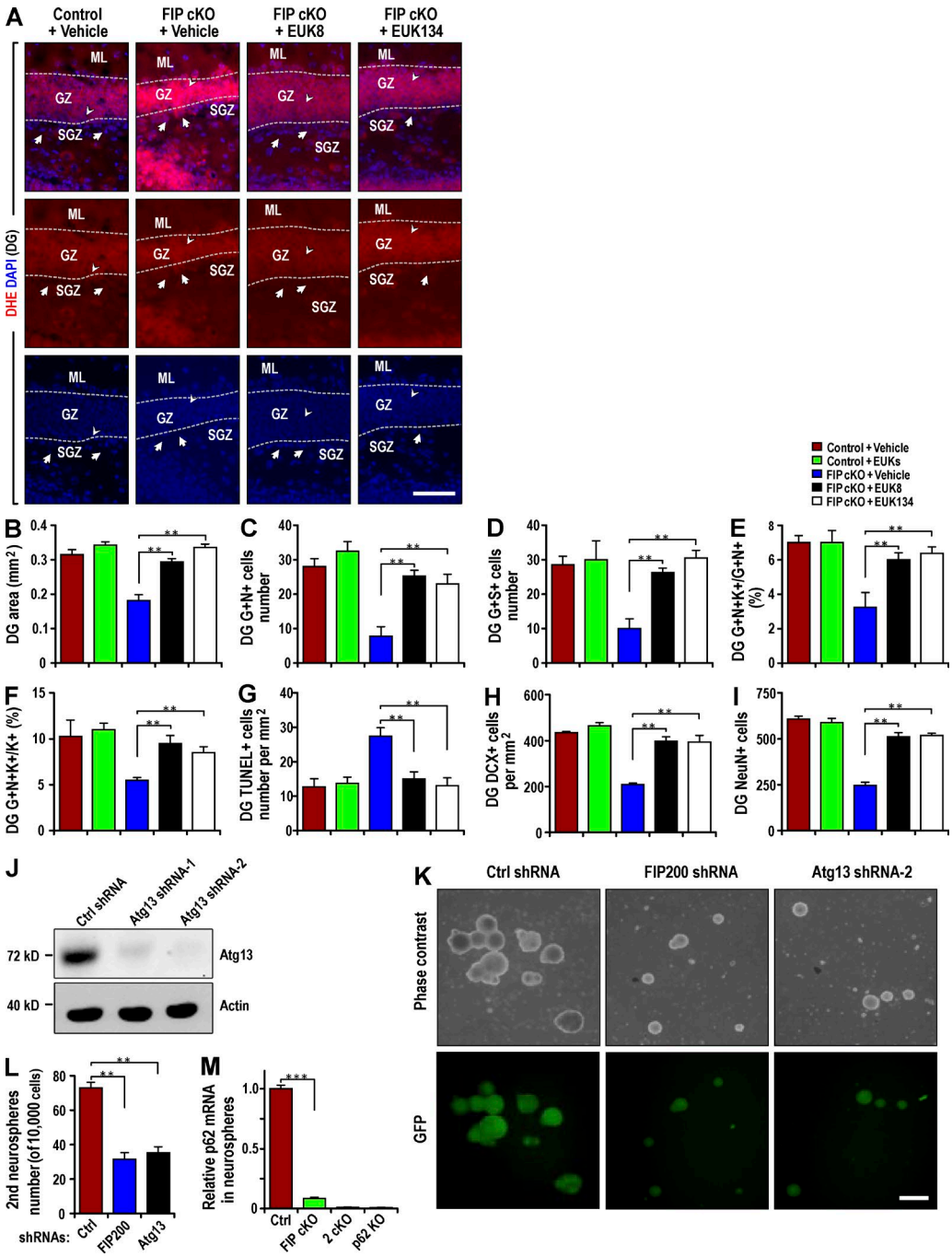

Figure S4. **SOD mimetics restore normal superoxide levels and rescue defective neural stem cells in the DG of *Fip200*^{GFAP} cKO mice, Atg13 knockdown decreases neurosphere formation of SVZ cells, and decreased p62 mRNA in Fip200-null neurospheres.** Ctrl and *Fip200*^{GFAP} cKO mice at P28 were treated with vehicle or EUK-8 and EUK-134 for 21 d as described in Materials and methods. (A) DHE and DAPI fluorescence in the DG of the mice. Arrows indicate SGZ cells and arrowheads indicate granular neurons. Dotted lines indicate the boundaries of the GZ (n = 4 mice each). (B) Mean ± SEM of the DG area per section from these mice are shown (n = 3 mice each). (C and D) Mean ± SEM of the GFAP$^+$Nestin$^+$ (C) and GFAP$^+$SOX2$^+$ (D) cells per section from the mice are shown (n = 4 mice each). (E and F) Mean ± SEM of the percentage of GFAP$^+$Nestin$^+$Ki67$^+$ of total Ki67$^+$ cells (E) or total GFAP$^+$Nestin$^+$ cells (F) in the SGZ of these mice are shown (n = 4 mice each). (G–I) Mean ± SEM of TUNEL$^+$ (G), DCX$^+$ (H) per square millimeter of DG area and NeuN$^+$ (I) cells per DG of the mice are shown (n = 4 mice each). (J) MEFs were infected with recombinant lentiviruses encoding Atg13 shRNA or a control shRNA. Three days after infection, lysates were prepared and analyzed by immunoblotting with antibodies as indicated. (K and L) Representative phase contrast and GFP images (K) and mean ± SEM of the number of neurospheres (L, with diameters >40 µm) from the SVZ cells of P28 Ctrl mice that had been infected with lentiviruses and cultured in the presence of puromycin (to enrich for infected cells, as the lentivirus vector contains a puromycin-resistant gene). (M) Mean ± SEM of the relative p62 mRNA levels (normalized to level in Ctrl mice) in neurospheres derived from mice as indicated (n = 3 mice each). Bars: (A) 50 µm; (K) 100 µm. ML, molecular layer. **, $P < 0.01$; ***, $P < 0.001$.

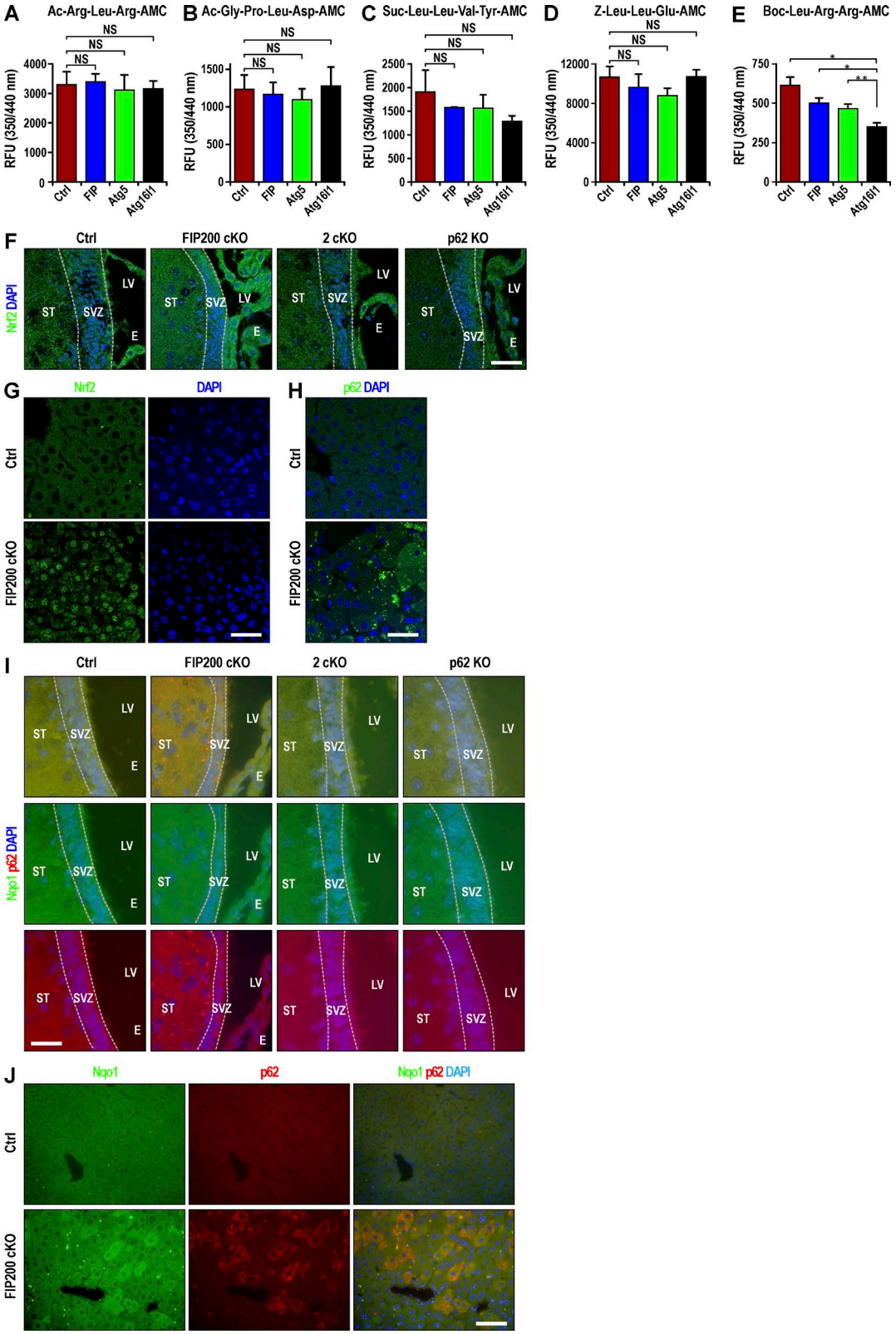

Figure S5. **Analysis of proteasome activity and activation of p62-Keap1-Nrf2 axis in neural stem cells of Ctrl, *Fip200*^{GFAP} cKO, *Atg5*^{GFAP} cKO, and *Atg16L1*^{GFAP} cKO mice.** (A–E) Lysates prepared from neurospheres of SVZ cells in Ctrl, *Fip200*^{GFAP} cKO, Atg5 cKO, and Atg16L1 cKO mice were measured for their proteasome activities using various substrates as indicated. Mean ± SEM from three independent experiments are shown. RFU, relative fluorescent unit. (F) Immunofluorescence of Nrf2 and DAPI in SVZ of Ctrl, *Fip200*^{GFAP} cKO, 2cKO, and p62 KO mice at P28. The dotted lines indicated the boundary of SVZ. (G and H) Immunofluorescence of Nrf2 (G) or p62 (H) with DAPI in the liver of Ctrl and Fip200f/f;Mx1-Cre mice after pIpC treatment. (I) Immunofluorescence of Nqo-1, p62 and DAPI in SVZ of Ctrl, *Fip200*^{GFAP} cKO, 2cKO, and p62 KO mice at P28. The dotted lines indicated the boundary of SVZ. (J) Immunofluorescence of Nqo1 and p62 with DAPI in liver of Ctrl and Fip200f/f;Mx1-Cre mice after pIpC treatment. E, ependymal layer; LV, lateral ventricle; ST, striatum. Bars: (F and I) 50 µm; (G, H, and J) 25 µm. *, $P < 0.05$; **, $P < 0.01$.